Morphology and histology of the mouthparts and gut system of *Macarorchestia remyi* (Schellenberg, 1950) (Amphipoda, Talitridae)

Morfología e histología de las piezas bucales y el sistema digestivo de *Macarorchestia remyi* (Schellenberg, 1950) (Amphipoda, Talitridae)

D. Davolos *, L. Pavesi, F. Accordi & E. De Matthaeis

Department of Biology and Biotechnology "Charles Darwin", Sapienza University of Rome, Viale dell'Università, 32, 00185 - Rome, Italy.

* Corresponding author: davolos.it@libero.it; Tel: +39 0649914956; Fax: +39 064958259

Recibido el 13 de septiembre de 2010. Aceptado el 15 de diciembre de 2010.

ISSN: 1130-4251 (2010), vol. 21, 151-178.

Special Issue: Amphipods: Trends in systematics and ecology (Guest editor: J. M. Guerra García).

Key words: Histology; Talitridae; *Macarorchestia*; foregut; midgut; hindgut.
Palabras clave: Histología, Talitridae, *Macarorchestia*, digestivo anterior, estomodeo, mesodeo; proctodeo.

ABSTRACT

Macarorchestia remyi lives in beached logs, where it makes its tunnels by eating the wood. Hence, this wood-feeding species has a peculiar diet compared with other Mediterranean talitrid amphipods. We carried out a morphological analysis of its mouthparts and a mainly histological investigation (transverse sections) of its gut regions (foregut, midgut and hindgut). The ectodermal foregut and hindgut regions are typically lined with cuticle, finely elaborated into various structures. Near the distal end of the oesophagus are the lateralia, provided with two rows of setae and several stout spines. The primary filter, including two parallel channels, is located ventrally in the first region of the foregut, while the secondary filter lies ventrally in the posterior foregut chamber, composed on each side of two longitudinal channels covered by densely arranged parallel setae. In the hindgut, the lining folded cuticle of the cylindrical epithelium shows unspecialized spines. In the endodermal midgut, the fine materials extracted from the upper foregut chambers through the filter systems are conveyed from the ventral channels to two pairs of ventrally located hepatopancreatic tubules; all these lobes, surrounding the midgut and partia-

lly the hindgut, are characterized by large vacuolated cells in their proximal regions. The midgut caeca includes the paired tubular pyloric caeca lateral to the secondary filter and a single caecum dorsal to the midgut. Two posterior caeca, originating in the distal part of the midgut, are located dorsolaterally and partially surround the hindgut. Finally, we observed layers of peritrophic membranes in the lumen of the midgut. In summary, the molar surface morphology appears to agree with the trend previously hypothesized for talitrid taxa with an increasing landward habitat and shifting toward a typical terrestrial diet. However, our data suggest that *M. remyi*, despite its particular feeding preference, shows no major differences in the main gut structures from other talitroid species. This relatively uniform morphology can be considered close to the ground pattern of the gammaridean amphipods, probably representing the early stage of Amphipoda evolution

RESUMEN

Macarorchestia remyi vive e troncos de la playa, donde hace túneles comiendo la madera. Por tanto, esta especie que ingiere madera tiene una dieta peculiar comparada con otros anfípodos talítridos del Mediterráneo. Llevamos a cabo un análisis morfológico de las piezas bucales y una investigación histológica (cortes transversales) de las regiones del digestivo (foregut, midgut and hindgut). Las regiones del hindgut y el foregut ectodérmico están cubiertas por cutícula, muy estructurada. Cerca del estremo final del esófago se encuentra la lateralia, provista por dos filas de sedas y varias espinas. El filtrado primario, incluyendo dos canales paralelos, se localiza centralmente en la primera región del foregut, mientras que el filtrado secundario se localiza centralmente en la cámara del foregut posterior, compuesta a cada lado por dos canales longitudinales cubiertos por sedas paralelas densas. En el hindgut, la cutícula del epitelio cilíndrico muestra espinas poco especializadas. En el midgut endodérmico, los materiales finos extraidos de las cámaras superiors del foregut, convergen de los canales ventrales en dos pares de túbulos del hepatopáncreas; todos estos lóbulos, rodeando al midgut y parcialmente al hindgut, se caracterizan por células vacuolazas en las regiones proximales. La caeca del midgut incluye un par de tubulos pilóricos laterales y un caecum simple dorsal en el midgut. Dos caeca posteriores, que se originan en la parte distal del midgut, se localizan dorsolateralmente y rodean parcialmente el hindgut. Finalmente, se observan capas de membranas peritróficas en el lumen del midgut. En resumen, la morfología de la superficie molar parece coincidir con la tendencia previamente hipotetizada para los talítridos, con tendencia al hábita terrestre y adopción de una dieta típicamente terrestre. Sin embargo, nuestros datos sugieren que *M. remyi*, a pesar de us prferencias particulares de alimentación, no muestra diferencias importantes con las estructuras principales del digestivo de otras especies de talítridos. Esta morfología relativamente uniforme pude ser considerada cercana al patrón basal de los gammaridos, representando probablemente una fase temprana en la evolución de los anfípodos

INTRODUCTION

Plant detritus flows into marine ecosystems mainly through rivers, and the lignocellulose can be used as a food resource by a wide range of wood-degrading invertebrates. Peracarid crustaceans, such as amphipods and isopods, play an important trophic role in the faunal community of the shoreline. *Macarorchestia remyi* (Schellenberg, 1950) is an amphipod species belonging to the family Talitridae. It lives in beached rotting logs, where it makes its tunnels by eating the wood (Pavesi & De Matthaeis, 2009). In addition, it ingests and digests plant detritus in the wood it inhabits. A gut content analysis showed that this amphipod is primarily a wood detritivore, with a minor role in its diet of macro-epiphytes (algae, etc.). Hence, *M. remyi* has a peculiar diet compared with other Mediterranean talitrid amphipods. In addition, the species has a semi-annual life cycle and seems to show stronger adaptations to terrestrial life than other Mediterranean members of the Talitridae that live on beaches (Pavesi & De Matthaeis, 2009).

Interest in *M. remyi* has recently been renewed. Given its association with the ephemeral habitat of stranded rotting logs, some Italian populations of *M. remyi* have been subjected to molecular studies based on mitochondrial DNA sequences, aimed at analysing the genetic structure of this peculiar detritivore species (Pavesi *et al*., 2011). Moreover, its degradation and digestion of wood tissues are currently under investigation by our group. Like other detritivore crustaceans, *M. remyi* presumably produce cellulases to digest plant detritus (Byrne *et al*., 1999), but the contribution of microbial enzymes to the hydrolysis of lignin and cellulose is still not completely known (Johnston *et al*., 2005; Davolos *et al*., 2010).

The distinctiveness of feeding on rotting wood raised the question of whether *M. remyi* has specialized structures in its digestive tract compared with other talitroid amphipod taxa. In other words, did the dietary preference modify the morphology of the gut regions of this amphipod or did the digestive tract morphology of this crustacean mainly depend on the superfamily phylogeny?

Therefore, we carried out a morphological analysis of the mouthparts and a mainly histological investigation (transverse sections) of the foregut, midgut and hindgut of *M. remyi* to provide a preliminary overview and to test our hypothesis. We also compared our findings on *M. remyi* with those on previously studied talitroid amphipods.

MATERIAL AND METHODS

Sampling

M. remyi specimens of both sexes were collected by hand each month on beached rotten wood at Principina a Mare (Grosseto), Tuscany, central Italy, from November 2006 to January 2007 and April 2008.

Morphology

For a basic macroscopic analysis of adult individuals of *M. remyi* (generally at the intermoult stage, mean length 6 mm for females and 7 mm for males, fixed in 80% ethanol), we examined longitudinal sections from dissected specimens under a Leica binocular microscope mounted with a Nikon digital camera. For light microscope observations, the mouthparts and gut regions were removed from ethanol-preserved specimens (or kept for at least 2 h in a fixative containing 40% formaldehyde in phosphate-buffered saline) and then processed for descriptions on an Olympus BX-51 microscope mounted with a digital camera.

Histology

To obtain *M. remyi* free of ingested materials and to avoid the circulation of fluids inside the hepatopancreas, specimens (adult individuals, in intermoult stage) were housed individually in 150 ml plastic tubs for 3 days without food. For the histological examination, the specimens were fixed for 6 h in Bouin's fluid (the pereopods were cut to allow adequate penetration of the fixative). The specimens were kept in 70% ethanol for 1 h and then in 80% ethanol overnight to clear the samples of Bouin's fluid. The day after, the specimens were dehydrated through a graded alcohol series at 4°C, cleared in histolemon (4 times, each 10 minutes) and finally embedded in paraffin wax at 60°C (including an overnight step, for better wax penetration). Transverse serial sections 6 μm thick were made with a microtome using a steel knife. The sections were then rehydrated and stained with haematoxylin-eosin (Mazzi, 1977). Histological sections were examined by bright field light microscopy and digitalized using a digital camera mounted on an Olympus BX-51 microscope.

RESULTS

Morphological analysis

The mouth of *M. remyi* is situated on the antero-ventral side of the cephalic region, bounded by the mouthparts. The mouthparts include two robust mandibles typically equipped with well calcified structures: the proximal or molar processes, a small articulate plate inserted close to the incisor and known as the lacinia mobilis, and the distal or incisor processes; between the molar and the lacinia mobilis are the accessory blades. In more detail, the configuration of the molars is broad, almost oval with a grinding surface harbouring a regular pattern of 18 transverse lamelliform ridges partially overlapping each other (Fig. 1A, B, C), while the sharp incisors bear two lateral and three dorsal teeth (Fig. 1A). The lacinia mobilis of the left mandible appears 4-dentated (Fig. 1A).

Light microscopy revealed that the digestive tract of *M. remyi* consists of three main divisions: foregut, midgut and hindgut. The foregut can be divided into an oesophagus, an anterior or "cardiac" stomach and a posterior or "pyloric" stomach. The oesophagus connects the mouth with the stomach, which reaches into the anterior part of the second pereonite. Near the distal end of the oesophagus are two paired structures known as lateralia, covered with several thin setae laterally and with two rows of stout spines medially (the internal row is formed by stronger, twice as long spines; Fig. 2A, B). All these projections are directed posterolaterally whilst striated muscles are inserted on the dorsal side of the lateralia (Fig. 2A).

Structural outgrowths of the foregut cuticle divide the stomach longitudinally into the dorsal chamber (in turn surmounted by a small chamber that posteriorly appears as paired channels; Fig. 3) and a ventral filter chamber region, including channels separated by an anterior and a posterior ventromedian ridge known as "inferomedianum" or "interampullary ridge" (Figs. 3-4). The dorsal chamber of the anterior stomach appears as an oval cavity leading into the smaller upper chamber of the posterior stomach, which in turn leads into the midgut. The storage cavity can contain ground plant detritus, while the ventral channels can hold fine organic particles extracted from the storage chamber through the primary and secondary filter system. The primary filter, located ventrally in the "cardiac" chamber, includes two parallel channels covered by long setae. The secondary filter, located in the "pyloric" chamber on the basis of the ventral ridge (Figs. 3-4), is composed on each side of two adjacent longitudinal channels (Figs. 3-4) opening caudally into the entrance of the hepatopancreatic ducts. The two filter channels are covered by dense, parallel setae laterally on the external side of the interampullary ridge (ca. 200, attached to each other

at regular intervals). The posterior inferomedianum is enclosed by paired folds, known as "supra-ampullary folds", covered by setae which face the secondary filter (Figs. 3-4).

The midgut runs from the dorsal chamber of the pyloric stomach and partially lies on the dorsal and lateral wall of the two pairs of large tubules or hepatopancreas (Figs. 6-16). The latero-ventrally located hepatopancreatic lobes begin in the anterior part of the second pereonite ventral to the stomach, where they appear fused medially ventral to the end of the secondary filter, and extend into the pleon segments. The diameter is largest on the second and third pereonite (Figs. 6-16). The hepatopancreas structures surround the midgut and partially the hindgut (one pair running for a longer tract than the other one; Figs. 14-16) and each can be divided into distal, medial and proximal zones.

In addition, there is a pair of pyloric tube-like caeca located anteriorly, lateral to the median folds of the secondary filter (Figs. 3-5), and a single tubular caecum dorsal to the midgut (Figs. 6, 8, 9).

Two posterior caeca, located dorsolaterally, originate at the posteriormost limit of the midgut (Figs. 14-15) and partially surround the hindgut; they appear as tubular structures, each divisible into distal, medial and proximal tracts (Figs. 14-24).

Histological investigations

We examined the ectodermal foregut and hindgut regions typically lined with cuticle. As expected, the cuticle is composed of a thin dense epicuticle, a thick lamellar exocuticle and a less structured endocuticle. A thin epithelial layer lies on the thick cuticle of the foregut, which is finely elaborated into various structures (described above). In the lower chamber of the posterior stomach, the cuticle forms the double structure of the secondary filter (Figs. 3-4). Externally, this filter consists, on each side (lateral sides of the posterior region of the inferomedianum; Figs. 3-4), of an outer grating of elongated setae and an inner setal row comprising longer filter bars where each seta appears to be equidistant to the next. The inner filtration setae form, on each side, a wider longitudinal channel (Figs. 3-4). Moreover, the setae covering the paired "supra-ampullary folds" face the secondary filter (Figs. 3-4). The developed extrinsic striated musculature of the foregut occurs on both the dorsal and ventral side of the stomach, and some of it is related to the filter zone (Fig. 3).

In transverse section, the anterior midgut of *M. remyi* shows a simple epithelium, while at the posterior regions the midgut epithelium appears pseudostratified and more elaborate (Figs. 6-13). The midgut cells are

generally cubical, approximately 7 μm in height, with central nuclei and a basophilic cytoplasm (Figs. 6-13). Layers of peritrophic membranes are observed in the lumen of the midgut, encompassing mainly the posterior regions of the midgut, and they appear to be produced by delamination of the apical membranes of cells of the midgut (Figs. 11-12). In the end part of the midgut (at the midgut-hindgut junction), two different cell types are present in the dorsal and ventral epithelium, respectively (Figs. 14-15). The dorsal cells (ca. 20 μm long) are columnar with a large oval nucleus, while the ventral cells are cuboidal (ca. 5 μm) with large round nuclei (Figs. 14-15); a substance, appearing granular and basophilic, is located in the lumen (Figs. 14-15; see below).

The paired pyloric caeca, lateral to the secondary filter (Figs. 3-5), contain cells (ca. 5-8 μm) with a large round or oval nucleus in a basophilic cytoplasm, densely arranged around a very narrow lumen (Fig. 5).

The epithelium of the dorsal anterior caecum, dorsal to the midgut (Figs. 6, 8, 9), appears simple, generally folded and formed by cubical and apparently undifferentiated cells with round or oval nuclei (characterised by the presence of nucleoli), which occupy most of the basophilic cytoplasm (Figs. 6, 8, 9).

Each hepatopancreatic structure is surrounded by a network of muscle fibres (circular and small-diameter longitudinal muscle fibres) and presumed connective tissue (Figs. 6-18). The hepatopancreatic tubules are lined by a pseudostratified epithelium consisting of different cell types. The distal part of each tubule is characterized by non-vacuolated cuboidal and undifferentiated cells (known as E-"Embryonic" cells) with a prominent round nucleus (containing nucleoli) occupying most of the basophilic cytoplasm (Figs. 13-18). The E-cells are densely arranged around a narrow duct, with the apical region apparently showing a thin brush border towards the lumen space (Figs. 16-18). The epithelium of the remaining tubules (medial and proximal zones) is characterized by two similar cuboidal cells, F-cells (called Fibrillenzellen due to their conspicuous striated appearance, due to a well-developed rough endoplasmic reticulum) and R-cells (the commonly accepted term for resorptive cells) with an apical region in the lumen, a round nucleus towards the central region of the cell and a basophilic cytoplasm (Fig. 7; Figs. 10-11). Large cells (B-"Blisterlike" cells), common in the proximal region of the hepatopancreas, have a large, filled vacuole encompassed by a thin layer of cytoplasm and a nucleus restricted to the basal region of the cell (Fig. 7; Figs. 10-11). Vacuolated B-cells are arranged along the lumen, occupying approximately three-quarters of the internal boundaries (Fig. 7; Figs. 10-11). The solid contents and fluids inside the vacuoles can be liberated into the lumen of the caecum by apocrine,

holocrine and merocrine secretion, and material from the hepatopancreatic lumen can be taken in by pinocytotic activity at the apical membrane of the B-cells (Fig. 7; Figs. 10-11). Small cells (known as M-"Midget" cells), characterized by no direct contact with the lumen, a basophilic cytoplasm and a round or oval central nucleus that appears surrounded by a thin film of cytoplasm (Fig. 7), appear to be scattered throughout the length of the hepatopancreatic tubules (e.g. Figs. 6-12).

In the hindgut, the lining folded cuticle of the cylindrical uni-layered epithelium (ca. 20 μm) presents an increasing number of longitudinal unspecialized spines (Figs. 16-18). The elongate cells of the hindgut epithelium are characterized by direct contact with the lumen, a basophilic cytoplasm and a large round or oval central nucleus with several nucleoli. Extracellular material, appearing basophilic and granular, is distributed over the entire surface of the hindgut lumen, among and around the spines, completely enveloping the inner layer of this gut tract (Figs. 16-18). Presumed myoepithelial cells or muscle fibres located behind the cylindrical epithelium encompass the posterior regions of the hindgut (e.g. Fig. 21), suggesting that they act to achieve defecation.

Each of the two posterior caeca of the midgut, situated dorsolaterally and partially surrounding the hindgut (Figs. 14-24), occur as tubular structures and can be divided into different zones. They appear to be encompassed by laminar tissue and by a meshwork of longitudinal and circular muscles, while the epithelium consists of small cuboidal cells with a high nucleus/cytoplasm ratio (e.g. Fig. 24).

DISCUSSION

The superficial features of *M. remyi* generally correspond to the original brief description of the species (Schellenberg, 1950), as well as to another short description with supplementary figures by Ruffo (1993, fig. 506). In the latter work, Ruffo moved *Orchestia remyi* into the genus *Macarorchestia* Stock, 1989. However, since the diagnosis of the genus *Macarorchestia* was based only on a single species, *Macarorchestia martini*, collected in a cave in the Azorean islands and considered either a recent troglobion or a trogloxenous form (Stock, 1989), some discrepancies with *M. remyi* can be expected. Among the inconsistencies we observed, the flagellum of antenna 1 is formed by 5 segments instead of 3, and the pleopodal rami have more than 1 segment (data not shown). Regarding the mouthparts of *M. remyi*, according to our observations the lacinia mobilis of the left mandible is 4-dentated (Fig. 1A) in accordance with Stock & Abreu's observations

(1992, fig. 33) of *M. remyi* specimens from Corsica (type locality), but in contrast to the lacinia mobilis equipped with 5 teeth of the congeneric *M. martini* (Stock, 1989). Future detailed taxonomic work needs to redefine the description of the generic structures based on all the available information for taxa belonging to the genus *Macarorchestia*.

Recent studies have shown that modifications of mandibular morphology in gammarid amphipods can be explained by the feeding habits and thus are indicative of their trophic ecology (Mekhanikova, 2010). The mandibles of *M. remyi*, equipped with sharp incisors and with a large molar surface formed by a relatively low ridge number (Fig. 1A, B, C), show a morphological adaptation for grinding the cellulose matrix. Our main observation for *M. remyi* appears to agree with the trend (a decreased number of spine ridges) hypothesized for the molar processes in talitrid taxa with an increasing landward habitat and shifting toward a typical terrestrial diet (Johnston *et al*., 2004).

Moreover, in *M. remyi* a grinding function of the lateralia can be inferred from the presence of striated muscles on their dorsal side and the rich supply of cuticular structures on the ventral face. In particular, ingested wood particles might be further ground by the rows of serrated spines with remarkably sharp edges (Fig. 2A, B), while the posteriorly directed thick spines may indicate their function as a detritus conveyer (Fig. 2A, B). It was recently shown that the morphology of the spines of the lateralia in some gammarid amphipods could be related to the food consumed (Mekhanikova, 2010). A previous electron microscopic study of the stomach of the talitrid amphipods *Orchestia cavimana* (a European semi-terrestrial species that requires revision according to a molecular study of Ketmaier & De Matthaeis (2010)) and *Arcitalitrus sylvaticus* (an Australian terrestrial species) showed common features of the lateralia, indicated as crushing structures (Strus & Storch, 2004). Unfortunately, we could not make a comparison with the terrestrial talitrid amphipod *Keratroides vulgaris* (which feeds on decaying leaf litter) due to the absence of information on the lateralia in this Australian species (Johnston *et al*., 2004).

The stomach (mainly the anterior part) of *M. remyi* appears to be an extensible storage cavity (see Coleman, 1991) in which contraction of the extrinsic muscles of the foregut cuticle can help mix plant detritus with hepatopancreatic enzymes. As suggested for other talitrids (Strus & Storch, 2004), the role of the dorsal cavity in this process remains to be elucidated for *M. remyi*. However, wood litter may be partially digested by bacteria and microfungi present both in the rotting vegetation prior to ingestion and in the hepatopancreas (Davolos *et al*., 2010), with microbial enzymes contributing to hydrolysis of wood litter formed by lignin, cellulose and xylan polymers.

Recently, Davolos *et al*. (2010) demonstrated that bacteria remained after starvation periods in empty hepatopancreatic tubules of *M. remyi*, suggesting the occurrence of a resident bacterial community (presumably symbionts). Similar results were recently reported for the homologous tubules of terrestrial isopods (see Zimmer, 2002 and literature therein; Wang *et al*., 2007). Our future molecular studies will focus on understanding the roles, if any, of these bacteria in degrading polysaccharides and other biopolymers.

The complex double structure of the filter system (Figs. 3-4) ensures that the small ground wood particles, probably partly digested, pass into the hepatopancreas, carrying the larger and harder plant residuals towards the midgut. The width of the longitudinal channels in the foregut filter systems of *M. remyi* could be related to its detritivorous diet. Further morphological studies on talitrid species (approximately 250 species distributed in about 50 genera), particularly those that have colonized terrestrial habitats (adding to similar data obtained from a previous study; Johnston *et al*., 2004), will be useful to indicate whether the width of the longitudinal channels and the space between setae of the filter systems are related to the diet.

The endodermal midgut epithelium of *M. remyi* is composed mainly of a single small cell type and, as generally described in crustaceans, can be considered active in the regulation of water flux and ion transport (Icely & Nott, 1992). Moreover, some authors have reported that in crustacean groups the midgut epithelium can produce peritrophic membranes (Brunet *et al*., 1994; Martin *et al*., 2006). In *M. remyi*, we observed presumed peritrophic membranes (Figs. 6-13), mainly encompassing the posterior regions of the midgut, which appear to be produced by delamination of the apical membranes of cells of the midgut. Although the function of peritrophic membranes in the lumen of the midgut in *M. remyi* is not clear, they probably separate ingested materials from the midgut epithelium but do not contribute to the digestion of vegetable fragments or to the absorption of food particles.

The characteristics of the cells observed in the hepatopancreas of *M. remyi* have been reported in almost all crustacean species studied (Brunet *et al*., 1994). Recently, Correia *et al*. (2002) examined the hepatopancreatic tubules of the amphipod *Gammarus locusta* and found its distal part dominated by E-cells while the proximal and medial regions were primarily characterized by B-cells and by F-cells and R-cells (closely resembling each other). Nevertheless, it is important to emphasize that the function of each cell type in the hepatopancreas of *M. remyi* (Figs. 6-15) is not yet well established. Nevertheless, the presence of a single large vacuole in B-cells of *M. remyi* indicates that they might be involved in the absorption of nutrients from the hepatopancreatic lumen. B-cells could also be responsible for intracellular digestion of the absorbed materials and secretion

of the vacuolar content into the lumen (e.g. Fig. 11). Indeed, amylase and other enzymes known to be involved in the hydrolysis of saccharides were previously detected in B-cells of talitrid amphipods (see Johnston *et al*., 2005 and literature therein), while alkaline phosphatase and esterases were absorbed by the B-cells through pinocytosis (see Johnston *et al*., 2005). R-cells of *M. remyi* may absorb nutrients from the lumen and function in the storage of lipid droplets and glycogen. Indeed, alkaline phosphatase is the major lipid that hydrolyses esterase on the microvilli of R-cells of talitrid amphipods (see Johnston *et al*., 2005 and literature therein). F-cells of *M. remyi*, which appeared to be cuboidal and resembled the R-cells (Fig. 7; Fig. 10), are probably involved in enzyme synthesis (Byrne *et al*., 1999; Correia *et al*., 2002). The absence of a substantial difference between F-cells and R-cells of other amphipods was mentioned by Icely & Nott (1984) and Correia *et al*. (2002).

The hindgut epithelium of *M. remyi* is lined by a thick cuticle and, as observed in other talitrid amphipods (Johnston *et al*., 2004), by longitudinal rows of spines (Figs. 16-23), probably to assist the movement and prevent back flow of undigested food (Icely & Nott, 1984). The presumed secretion detected on the hindgut lumen among and around the spines (Figs. 16-17; Fig. 21; Fig. 23) could lubricate the bolus as it passes towards the hindgut. Future studies are needed to elucidate the origin, chemical composition and function of this material located outside the hindgut epithelium.

Nine caeca arose from the midgut of *M. remyi*, seven from its anterior part and two from its posteriormost limit. Paired anterior caeca just lateral to the secondary filter press have been reported in hyalellid, gammarid and talitrid amphipods (Schmitz & Scherrey, 1983; Johnston *et al*., 2004). It should be noted that short anterior protuberances of the digestive glands that presumably are homologous structures of the anterior ventral caeca were found in *Caprella equilibra* and other species of caprellids (Keith, 1974). In *M. remyi*, the cells of the anterior pyloric caeca appeared compactly packed (Fig. 5). However, their function is still unclear, although they are probably not secretory as reported for the talitrid species analysed by Johnston *et al*. (2004).

The single anterior caecum of *M. remyi*, posterior to the filtration system and dorsal to the anterior part of the midgut where it originated (Figs. 6, 8, 9), does not have a defined function, but we believe it could be involved in the processes of absorption and digestion, albeit limited in comparison with the hepatopancreas (Icely & Nott, 1984). The fine structure of the epithelium and histochemical studies can show tissue characteristics indicative of the cellular function (Icely & Nott, 1985). Remarkably, anterior caeca are present in all amphipods (see Johnston *et al*., 2004), generally as

dorsal paired caeca (Keith, 1974; Icely & Nott, 1984) but also as a single caecum in the hyalellid amphipod *Hyalella azteca* (Schmitz & Scherrey, 1983), *M. remyi* (present study) and other talitrid species (Johnston *et al*., 2004), suggesting a peculiarity of Talitroidea.

The two posterodorsal caeca in *M. remyi* (Figs. 14-24), originating from the posterior part of the midgut (Figs. 14-15), could be considered the primary sites of secretory process (Schmitz & Scherrey, 1983) and of water and calcium fluxes during the moult cycle (Graf *et al*., 1992 and references therein). In *O. cavimana*, a calcium-binding ability of the protein Orchestin, synthesized by the cells of the posterodorsal caeca, was confirmed during moulting cycles for the cyclical biomineralization of the calcified cuticle (Hecker *et al*., 2004 and references therein).

In summary, our data suggest that, despite its particular feeding preference, *M. remyi* shows no major differences in main gut anatomy from other talitrid species; hence, the morphology strongly depends on the likely single evolutionary lineage of the Talitridae family within the Amphipoda (see recent advances made by mitochondrial sequence and gene rearrangement analyses; Davolos & Maclean, 2005; Davolos *et al*., 2005a, 2005b; Villacorta *et al*., 2008; Kilpert & Podsiadlowski, 2010 and literature therein; Ito *et al*., 2010). According to this hypothesis, the conservative structure of the digestive tract morphology reported for the Talitroidea (e.g. the presence of a single anterior dorsal caecum) is related to the monophyletic history of this superfamily. On a larger phylogenetic scale, the digestive structure of talitroid amphipods, including the presence of anterior lateral midgut caeca (Figs. 3-5), conforms to the plan exhibited by gammaridean amphipods (Icely & Nott, 1984) and thus can be associated with a likely plesiomorphic gut anatomy in this suborder (see Kobusch, 1998).

On the other hand, Coleman (1990) found differences in anatomical and morphological features of the gammaridean *Parandania boecki*, a specialist that feeds on Cnidaria. Another study by the same author (1994) showed a reduced filter zone and consequently modification of the midgut caeca in pelagic and food-specialist hyperiid amphipods in comparison with the general condition of gammaridean amphipods. Modifications in the digestive tract in highly derived cyamid amphipods have been assumed to be related to their parasitic habits (Keith, 1974). Therefore, the possibility that dietary preference has been an important evolutionary factor in modifying the digestive tract morphology is valid at least for present-day amphipods that are highly specialized in their food consumption (Icely & Nott, 1992).

Finally, our results show that, as in the major amphipod lineages (Wirkner & Richter, 2007), the haemolymph system of *M. remyi* comprises a single-chambered dorsal heart, which is continued in the body axis by the

anterior and posterior aortae (Figs. 6-24). However, a detailed description of the haemolymph vascular system of *M. remyi* (beyond the scope of this paper) will require further examination.

CONCLUSIONS

The molar surface morphology of *M. remyi* appears to agree with the trend previously hypothesized for talitrid taxa with an increasing landward habitat and shifting toward a typical terrestrial diet. Nevertheless, our morphological and histological results suggest that the main gut anatomy of *M. remyi* shows no major differences from the general digestive tract plan inferred for previously examined talitroid amphipods. Hence, the conservative digestive tract morphology of *M. remyi* appears to be strongly related to the monophyletic history of the superfamily Talitroidea. This relatively uniform morphology can be considered close to the ground pattern of the gammaridean amphipods, probably representing the early stage of Amphipoda evolution.

ACKNOWLEDGEMENTS

The authors appreciate the valuable comments and suggestions provided by an anonymous reviewer of the manuscript.

REFERENCES

Brunet, M.; Arnaud, J. & Mazza, J. 1994. Gut structure and digestive cellular processes in marine Crustacea. *Oceanography and Marine Biology: an Annual Review*, 32: 335-367.

Byrne, K. A.; Lehnert, S. A.; Johnson, S. E. & Moore, S. S. 1999. Isolation of a cDNA encoding a putative cellulase in the red claw crayfish *Cherax quadricarinatus*. *Gene*, 239: 317-324.

Coleman, C. O. 1990. Anatomy of the alimentary canal of *Parandania boecki* (Stebbing, 1888) (Crustacea, Amphipoda, Stegocephalidae) from the Antarctic Ocean. *Journal of Natural History*, 24: 1573-1585.

— 1991. Comparative fore-gut morphology of Antarctic Amphipoda (Crustacea) adapted to different food sources. *Hydrobiologia,* 223: 1-9.

— 1994. Comparative anatomy of the alimentary canal of hyperiid amphipods. *Journal of Crustacean Biology*, 14: 346-370.

Correia, A. D.; Pereira, A. L.; Costa, M. H. & Carrapiço, F. 2002. Functional anatomy of the midgut gland of *Gammarus locusta* (Crustacea: Amphipoda). *Journal of the Marine Biological Association of the UK*, 82: 201-204.

Davolos, D. & Maclean, N. 2005. Mitochondrial COI–NC–COII sequences of talitrid amphipods (Crustacea). *Heredity*, 94: 81-86.

Davolos, D.; Iannilli, V. & De Matthaeis, E. 2005a. *Analysis on the mitochondrial region between the COI and COII genes in Crustacea*. The Sixth International Crustacean Congress, Symposium on the Phylogeny of Crustacea. University of Glasgow, Glasgow, Scotland, UK. 18-22 July 2005.

Davolos, D.; Iannilli, V. & De Matthaeis, E. 2005b. *Molecular analysis on the mitochondrial COI-tRNA^{LeuUUR}-COII region in* Gammarus aequicauda *(Amphipoda, Gammaridae).* First Congress of Italian Evolutionary Biologists, University of Ferrara, Ferrara, Italy. 24-26 August 2005.

Davolos, D.; Pavesi, L.; Pietrangeli, B. & De Matthaeis, E. 2010. *Assessment of bacteria in the midgut glands of talitrid amphipods by fluorescence microscopy and molecular approaches.* XIVth International Colloquium on Amphipoda. University of Seville, Seville, Spain. 13-18 September 2010.

Graf, F. & Meyran, J. C. 1992. Neurosecretory cells in the posterior caeca of the amphipods *Orchestia* and *Niphargus*: ultrastructural characterization. *Italian Journal of Zoology*, 59: 49-55.

Hecker, A.; Quennedey, B.; Testenière, O.; Quennedey, A.; Graf, F. & Luquet, G. 2004. Orchestin, a calcium-binding phosphoprotein, is a matrix component of two successive transitory calcified biomineralizations cyclically elaborated by a terrestrial crustacean. *Journal of Structural Biology*, 46: 310-324.

Icely, J. D. & Nott, J. A. 1984. On the morphology and fine structure of the alimentary canal of *Corophium volutator* (Pallas) (Crustacea: Amphipoda), *Philosophical Transactions of the Royal Society of London B*, 306: 49-78.

— 1985. Feeding and digestion in *Corophium volutator* (Crustacea: Amphipoda). *Marine Biology*, 89: 183-195.

— 1992. Digestion and absorption: digestive system and associated organs. In: Harrison, F. W. and Humes, A. G. (Eds). *Microscopic anatomy of invertebrates: Decapod, Crustacea.* 10: 147-201. Wily-Liss Inc., N.Y.

Ito, A.; Aoki, M. N.; Yokobori, S.; Wada, H. 2010. The complete mitochondrial genome of *Caprella scaura* (Crustacea, Amphipoda, Caprellidea), with emphasis on the unique gene order pattern and duplicated control region. *Mitochondrial DNA*, 21: 183-190.

Johnston, M. D.; Johnston, D. J. & Richardson, A. M. M. 2004. Mouthpart and digestive tract structure in four talitrid amphipods from a translittoral series in Tasmania. *Journal of the Marine Biological Association of the UK*, 84: 717-726.

— 2005. Digestive capabilities reflect the major food sources in three species of talitrid amphipods. *Comparative Biochemistry and Physiology*, *Part B*, 140: 251-257.

Keith, D. E. 1974. A comparative study of the digestive tracts of *Caprella equilibra* Say and *Cyamus boopis* Lütken (Amphipoda, Caprellidea). *Crustaceana*, 26: 127-132.

Ketmaier, V. & De Matthaeis, E. 2010. Allozymes and mtDNA reveal two divergent lineages in *Orchestia cavimana* (Amphipoda: Talitridae). *Journal of Crustacean Biology*, 30: 307-311.

Kilpert, F., & Podsiadlowski, L. 2010. The mitochondrial genome of the Japanese skeleton shrimp *Caprella mutica* (Amphipoda: Caprellidea) reveals a unique gene order and shared apomorphic translocations with Gammaridea. *Mitochondrial DNA*, 21: 77-86.

Kobusch, W. 1998. The foregut of the Mysida (Crustacea, Peracarida) and its phylogenetic relevance. *Philosophical Transactions of the Royal Society of London B*, 353: 559-581.

Martin, G. G.; Simcox, R.; Nguyen, A.; Chilingaryan, A. 2006. Peritrophic membrane of the penaeid shrimp *Sicyonia ingentis*: structure, formation, and permeability. *The Biological Bulletin*, 211: 275-285.

Mazzi, V. 1977. *Manuale di tecniche istologiche e istochimiche*, Piccin Editore, Padova, Italy, 750 pp.

Mekhanikova, I. V. 2010. Morphology of mandible and lateralia in six endemic amphipods (Amphipoda, gammaridea) from Lake Baikal, in relation to feeding. *Crustaceana*, 83: 865-887.

Pavesi, L. & De Matthaeis, E. 2009. Life history of the amphipod *Macarorchestia remyi* (Schellenberg, 1950) on a Tyrrhenian sandy beach, Italy. *Hydrobiologia*, 635: 171-180.

Pavesi, L.; Ketmaier, V.; Tiedemann, R. & De Matthaeis, E. 2011. Population genetics and phylogeography of the sandhopper *Macarorchestia remyi* (Schellenberg, 1950) (Amphipoda, Talitridae) based on COI sequence data. *Zoological Studies*, 50: 220-229.

Ruffo, S. 1993. Genus *Macarorchestia* Stock; *Macarorchestia remyi* (Schellenberg, 1950). En: Ruffo, S. (Ed). *The Amphipoda of the Mediterranean. Part 3. Gammaridea (Melphidippidae to Talitridae), Ingolfiellidea, Caprellidea*. 13: 738-740. Mémoires de l'Institut océanographique, Monaco.

Schellenberg, A. 1950. Subterrane Amphipoden korsikanischer Biotope. *Archiv für Hydrobiologie*, 44: 325-332.

Schmitz, E.H. 1967. Visceral anatomy of *Gammarus lacustris lacustris* Sars (Crustacea: Amphipoda). *American Midland Naturalist,* 78: 1-54.

Schmitz, E.H. & Scherrey, P.M. 1983. Digestive anatomy of *Hyalella azteca* (Crustacea, Amphipoda). *Journal of Morphology*, 175: 91-100Stock, J.H. 1989. A new genus and species of Talitridae (Amphipoda) from a cave in Terceira, Azores. *Journal of Natural History*, 23: 1109-1118.

Stock, J.H. & Abreu, A.D. 1992. Talitridae (Crustacea, Amphipoda) from non-marine habitats in Madeira. *Boletim do Museu Municipal do Funchal*, 44: 115-129.

Strus, J. & Storch, V. 2004. Comparative electron microscopic study of the stomach of *Orchestia cavimana* and *Arcitalitrus sylvaticus* (Crustacea: Amphipoda). *Journal of Morphology*, 9: 340-346.

Villacorta, C.; Jaume, D.; Oromí, P. & Juan, C. 2008. Under the volcano: phylogeography and evolution of the cave-dwelling *Palmorchestia hypogaea* (Amphipoda, Crustacea) at La Palma (Canary Islands). *BMC Biology*, 31, 6: 7.

Wang, Y.; Brune, A. & Zimmer, M. 2007. Bacterial symbionts in the hepatopancreas of isopods: diversity and environmental transmission. *FEMS Microbiology Ecology*, 61: 141-152.

Wirkner, C.S. & Richter, S. 2007. Comparative analysis of the circulatory system in Amphipoda (Malacostraca, Crustacea). *Acta Zoologica* (Stockholm), 88: 159-171.

Zimmer, M. 2002. Nutrition in terrestrial isopods (Isopoda: Oniscidea): an evolutionary-ecological approach. *Biological Reviews of the Cambridge Philosophical Society*, 77: 455-493.

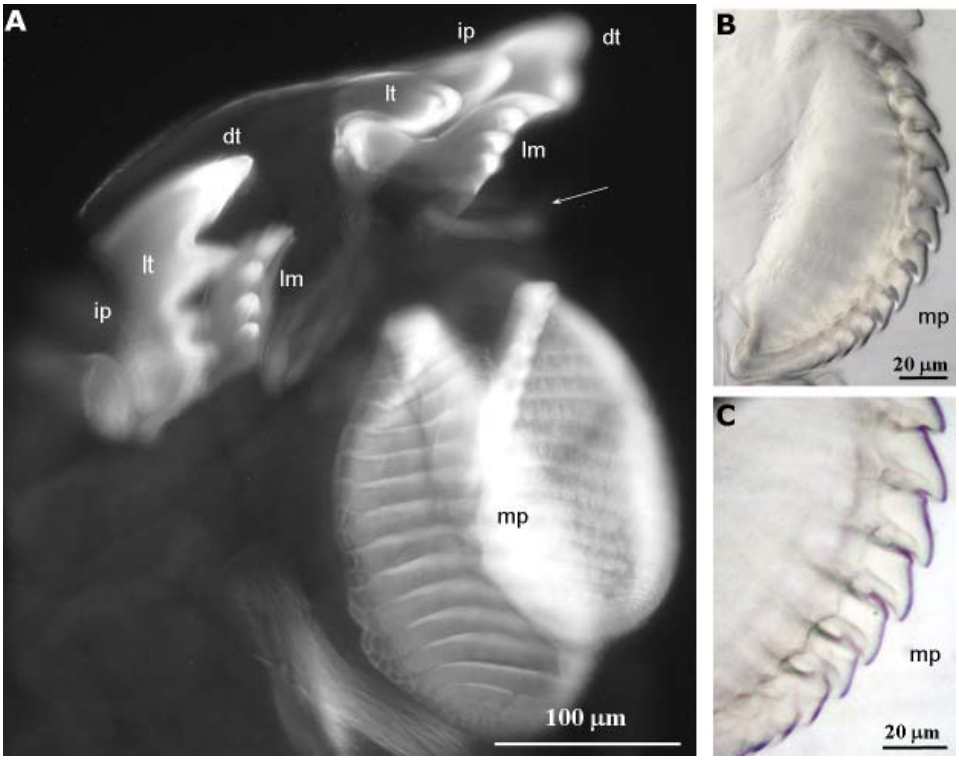

Fig. 1.—(A) Micrograph of the left mandible of an adult male of *M. remyi* in the premoult period. Note the new well-developed cuticle under the old one. The arrow indicates a setal tuft (not in focus). (B, C) Lateral views of the molar processes. dt, dorsal teeth; ip, incisor processes; lm, 4-dentate lacinia mobilis; lt, lateral teeth; mp, molar processes.

Fig. 1.—(A) Micrografía de la mandíbula izquierda de un macho adultod de *M. remyi* en el periodo de premuda. Se aprecia la nueva cutícula bien desarrollada por debajo de la antigua. La flecha indica un penacho de sedas. (B,C) Vistas laterales de los procesos molares. dt, dientes dorsales; ip, procesos incisivos; lm, lacinia con 4 dientes; lt, dientes laterals; mp, procesos molars.

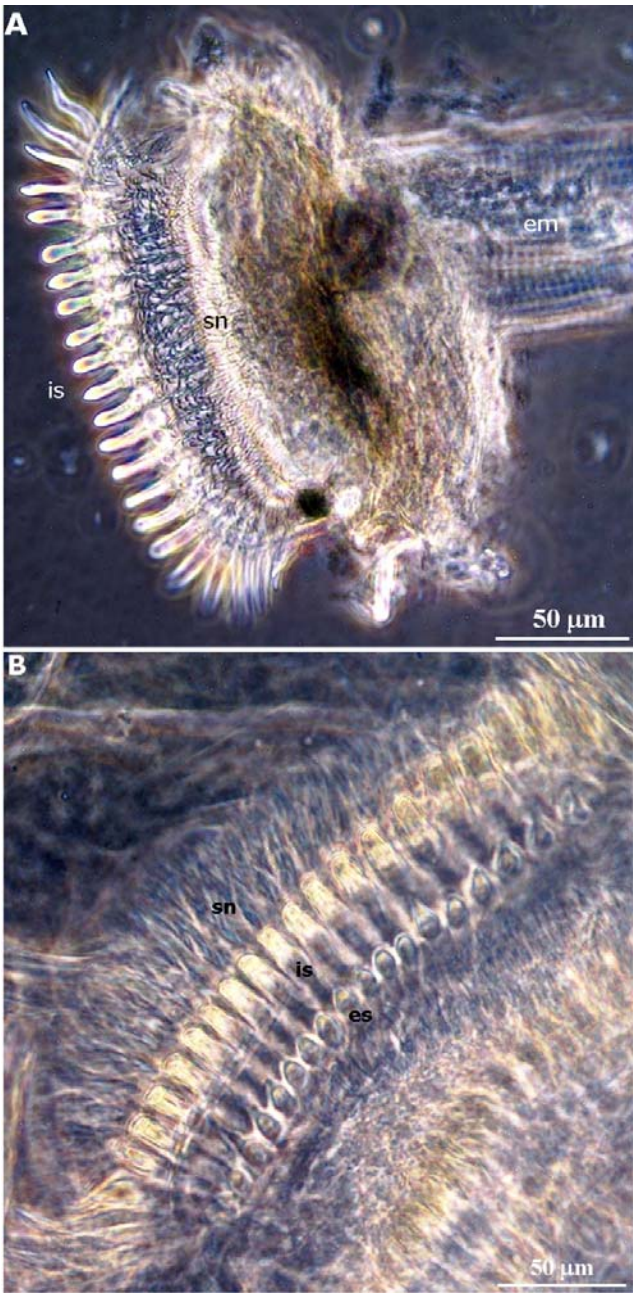

Fig. 2.—(A, B) Micrographs of the lateralia of an adult female of *M. remyi*. em, extrinsic muscles; es, external row of spines; is, internal row of spines; sn, spinules.
Fig. 2.—(A, B) Micrografías de la lateralia de una hembra adulta de *M. remyi*. em, músculos extrínsecos; es, fila externa de espinas; is, fila interna de espinas; sn, espínulas.

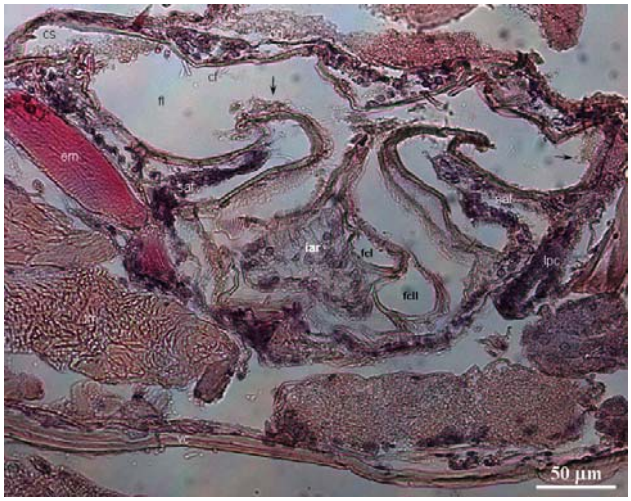

Fig. 3.—Transverse section of the secondary filter region of an adult male of *M. remyi*. Arrows point to plant detritus inside the lumen of the foregut. cf, cuticle of the foregut; cs, channel of the stomach; dd, dorsal diaphragm; em, extrinsic muscle; fcI, filter channel I; fcII, filter channel II; fe, foregut epithelium; fl, foregut lumen; iar, inferomedianum; lm, longitudinal muscles; lpc, lateral pyloric caecum; saf, supra-ampullary fold; vc, ventral cuticle.

Fig. 3.—Sección transversal de la región filtradora secundaria de un macho adulto de *M. remyi*. Las flechas señalan detritus vegetal dentro del lumen del estomodeo. cf, cutícula del estomodeo; cs, canal del estómago; dd, diafragma dorsal; em, músculo extrínseco; fcI, canal de filtrado I; fcII canal de filtrado II; fe, epitelio del estomodeo; fl, lumen del estomodeo; iar, inferomedianum; lm, músculos longitudinales; lpc, caecum pilórico lateral; saf, capa supra-ampular; vc, cutícula ventral.

Fig. 4.—Magnification of the two longitudinal channels. Arrows point to plant detritus inside the lumen of the foregut, arrowheads point to the setae of the supra-ampullary folds and of the secondary filter. cf, cuticle of the foregut; fcI, filter channel I; fcII, filter channel II; fl, foregut lumen; iar, inferomedianum; lpc, lateral pyloric caecum; saf, supra-ampullary fold.

Fig. 4.—Magnificación de los dos canales longitudinales. Las flechas señalan el detritus vegetal dentro del lumen del estomodeo, con las puntas de las flechas indicando las sedas de las capas supra-ampulares del segundo filtro. cf, cutícula del estomodeo; fcI, canal de filtrado I; fcII canal de filtrado II; fl, lumen del estomodeo; iar, inferomedianum; lpc, caecum pilórico lateral; saf, capa supra-ampular.

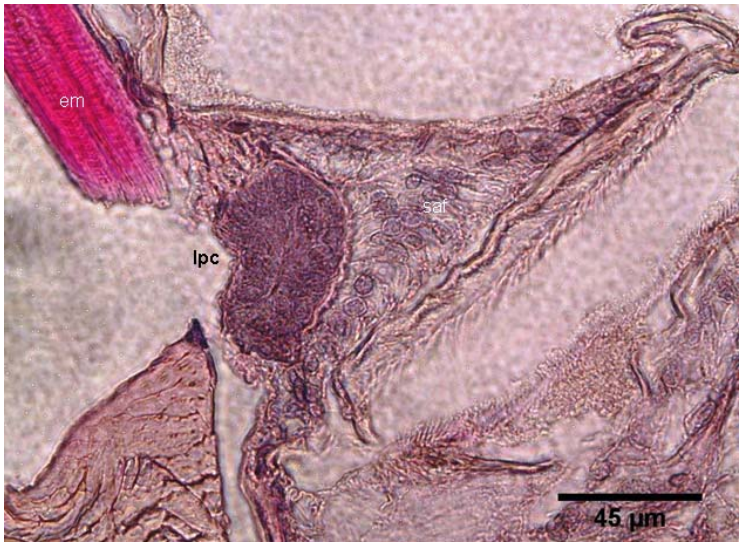

Fig. 5.—Magnification of the lateral pyloric caecum. em, extrinsic muscle; lpc, lateral pyloric caecum; saf, supra-ampullary fold. em, extrinsic muscle; lpc, lateral pyloric caecum; saf, supra-ampullary fold. Fig. 5.—Magnificación del caecum pilórico lateral; em, músculo extrínseco; lpc, caecum pilórico lateral; saf, capa supra-ampular.

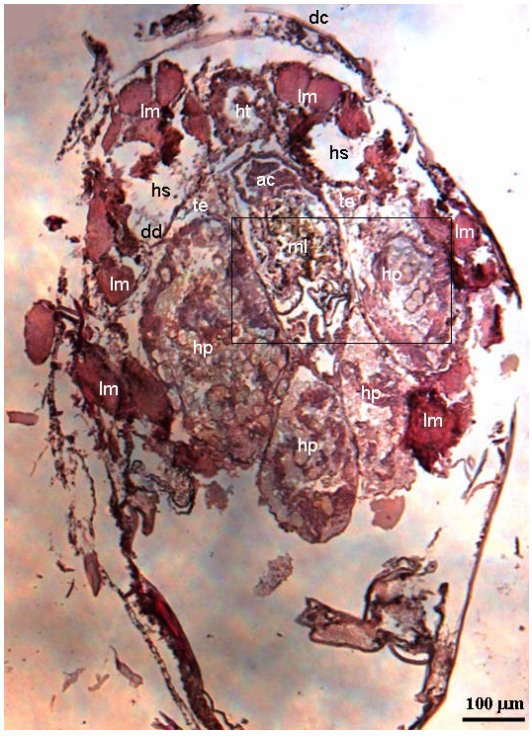

Fig. 6.—Transverse section of the anterior part of the midgut and of the proximal region of the hepatopancreas of an adult male of *M. remyi*. Note a pair of testes (proximal region) lateral to the midgut. ac, anterior caecum; dc, dorsal cuticle; dd, dorsal diaphragm; hp, hepatopancreas; ht, heart; lm, longitudinal muscles; ml, midgut lumen; te, testis.
Fig. 6.—Sección transversal de la parte anterior del mesodeo y de la region proximal del hepatopáncreas de un macho adulto de *M. remyi*. Se aprecian un par de testículos (región proximal) laterales al mesodeo. ac, caecum anterior; dc, cutícula dorsal; dd, diafragma dorsal; hp, hepatopáncreas; ht, corazón; lm, músculos longitudinales; ml, lumen del mesodeo; te, testículos.

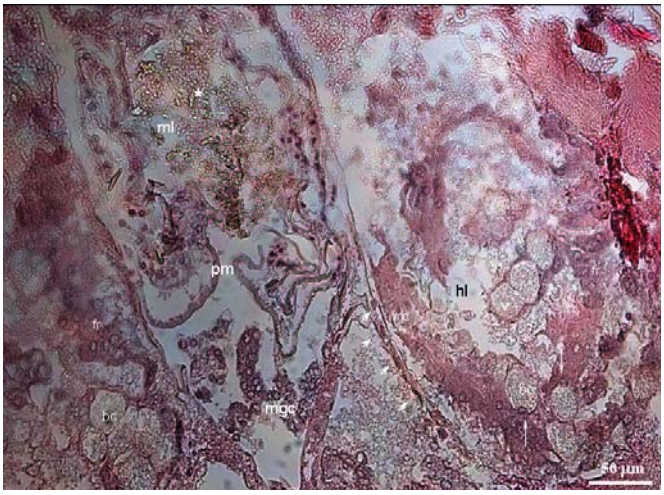

Fig. 7.—Magnification of the midgut and of the hepatopancreatic structures (see the rectangle within Fig. 6). Note the plant fragments (asterisk) in the midgut lumen. Arrows point to the nuclei of the B-cells, arrowheads point to the small-diameter longitudinal muscle fibres. ac, anterior caecum; bc, B-cells; fr, F/R-cells; hl, hepatopancreatic lumen; mc, M-cells; mgc, midgut cells; ml, midgut lumen; pm, peritrophic membranes; v, vacuole.

Fig. 7.—Magnificación del mesodeo y de las estructuras del hepatopáncreas (ver el rectángulo dentro de la Fig. 6). Se aprecian los fragmentos de plantas (asterisco) en el lumen del mesodeo. Las flechas señalan el núcleo de las células B, y las puntas de flecha indican las fibras musculares de pequeño diámetro. ac, caecum anterior; bc, células B; F/R; hl, lumen hepatopancreático; mc, células M; mgc, células del mesodeo; ml, lumen del mesodeo; pm, membranas peritróficas; v, vacuola.

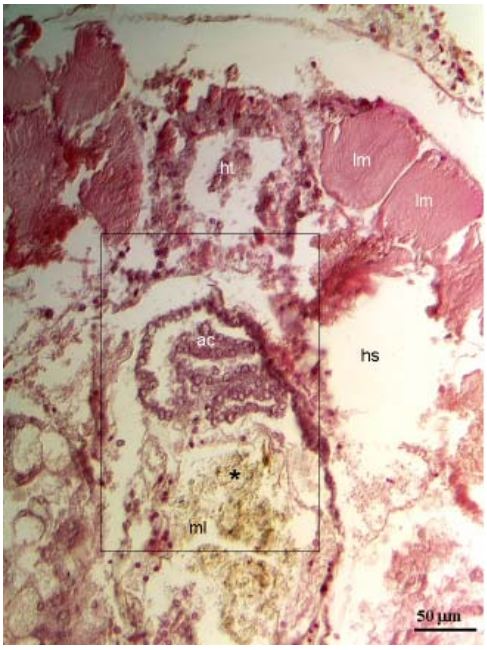

Fig. 8.—Magnification of the midgut and of the anterior caecum. The asterisk indicates plant fragments in the midgut lumen. ac, anterior caecum; hs, haemolymph sinus; ht, heart; lm, longitudinal muscles; ml, midgut lumen.

Fig. 8.—Magnificación del mesodeo y del caecum anterior. El asterisco indica los fragmentos de plantas en el lumen del mesodeo. ac, caecum anterior; hs, seno hemolinfático; ht, corazón; lm, músculos longitudinales; ml, lumen del mesodeo.

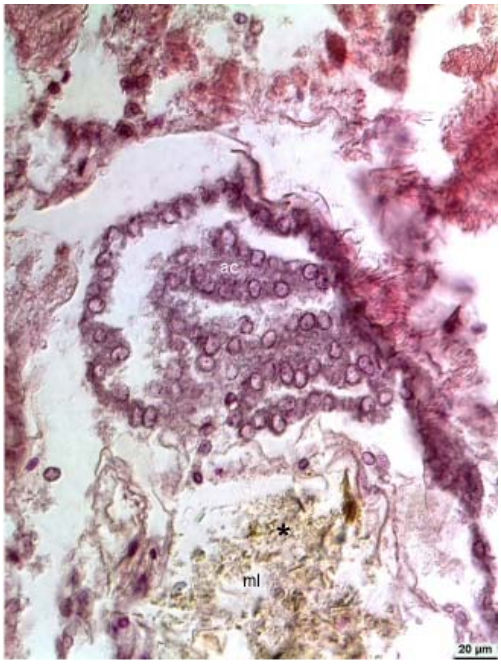

Fig. 9.—Magnification of the midgut and of the anterior caecum (see the rectangle within Fig. 8). The asterisk indicates plant fragments in the midgut lumen. ac, anterior caecum; ml, midgut lumen.
Fig. 9.—Magnificación del mesodeo y del caecum anterior (ver el rectángulo dentro de la Fig. 8). El asterisco indica los fragmentos de plantas en el lumen del mesodeo. ac, caecum anterior; ml, lumen del mesodeo.

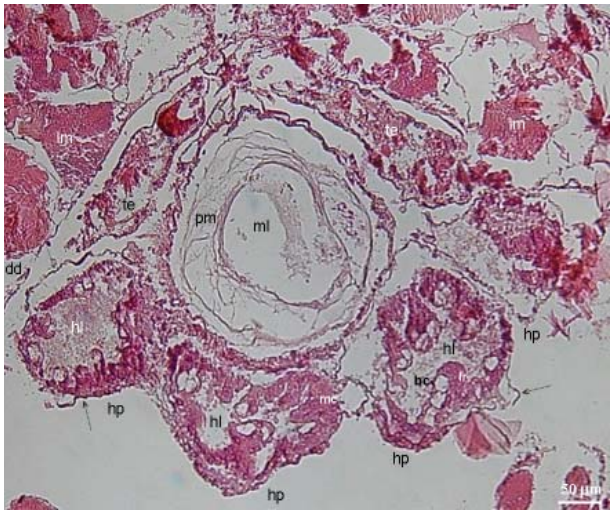

Fig. 10.—Histological section of the medial parts of the midgut and of the medial regions of the hepatopancreatic lobes in an adult male of *M. remyi*. Dotted arrows point to muscle fibres. bc, B-cells; dd, dorsal diaphragm; fr, F/R-cells; hl, hepatopancreatic lumen; hp, hepatopancreas; lm, longitudinal muscles; mc, M-cells; ml, midgut lumen; pm, peritrophic membranes; te, testis.
Fig. 10.—Sección histológica de la parte media del mesodeo y de las regiones medias de los lóbulos del hepatopáncreas en un macho adulto de *M. remyi*. Las flechas puntuadas apuntan a las fibras muculares. bc, células B; dd, diafragma dorsal; fr, células F/R; hl, lumen hepatopancreático; hp, hepatopáncreas; lm, músculos longitudinales; mc, células M; ml, lumen del mesodeo; pm, membranes peritróficas; te, testículo.

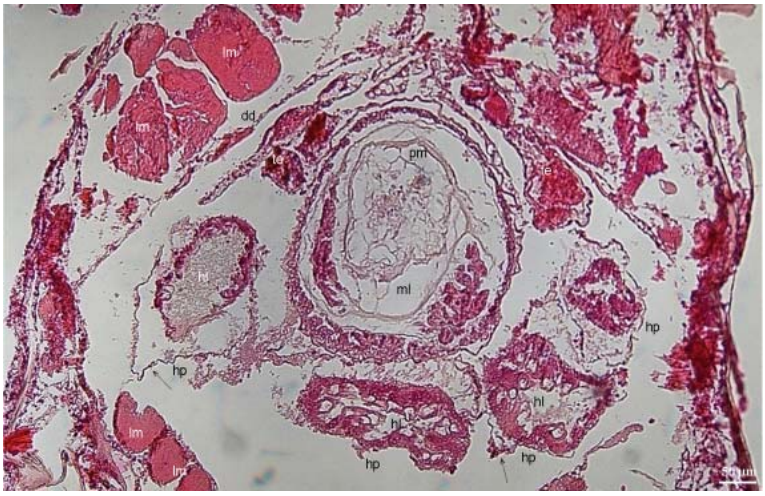

Fig. 11.—Other view of histological section of the medial parts of the midgut and of the medial regions of the hepatopancreatic lobes in an adult male of *M. remyi*. Dotted arrows point to muscle fibres. bc, B-cells; dd, dorsal diaphragm; fr, F/R-cells; hl, hepatopancreatic lumen; hp, hepatopancreas; lm, longitudinal muscles; mc, M-cells; ml, midgut lumen; pm, peritrophic membranes; te, testis.
Fig. 11.—Otra visión de la sección histológica de la parte media del mesodeo y de las regiones medias de los lóbulos del hepatopáncreas en un macho adulto de *M. remyi* Las flechas puntuadas apuntan a las fibras muculares. bc, células B; dd, diafragma dorsal; fr, células F/R; hl, lumen hepatopancreático; hp, hepatopáncreas; lm, músculos longitudinales; mc, células M; ml, lumen del mesodeo; pm, membranes peritróficas; te, testículo.

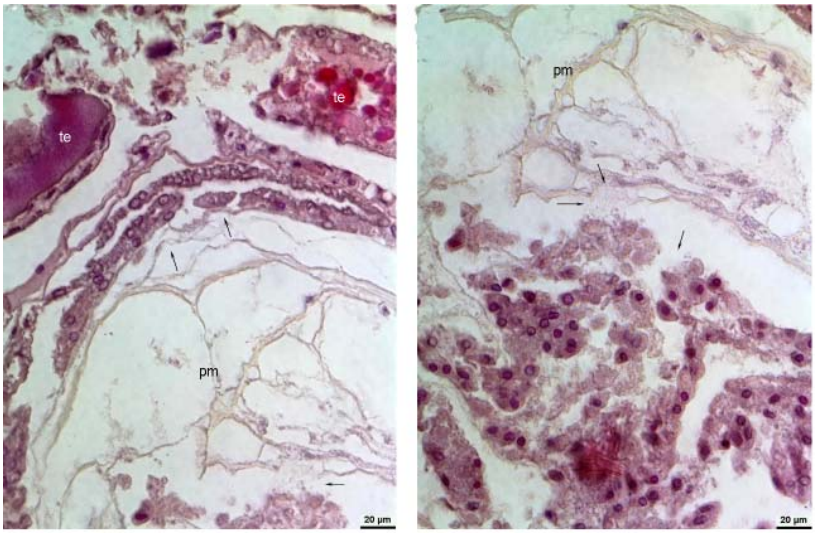

Fig. 12.—Magnification of the midgut. Arrows point to delamination of the midgut cells. pm, peritrophic membranes; te, testis.
Fig. 12.—Magnificación del mesodeo. Las flechas señalan la delaminación de las células del mesodeo. pm, membranas peritróficas; te, testículo.

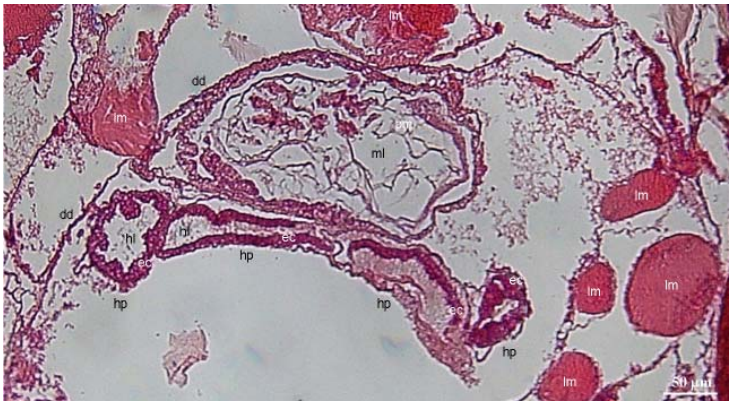

Fig. 13.—Transverse section of a posterior region of the midgut and of the distal parts of the hepatopancreas of an adult male of *M. remyi*. Note the absence of the gonads and of the posterior caeca. dd, dorsal diaphragm; ec, E-cells; hl, hepatopancreatic lumen; hp, hepatopancreas; lm, longitudinal muscles; ml, midgut lumen; pm, peritrophic membranes.

Fig. 13.—Sección transversal de la region posterior del mesodeo y de la parte distal del hepatopáncreas en un macho adulto de *M. remyi*. Se aprecia la ausencia de gónadas y de caeca posterior. dd, diafragma dorsal; ec, células E, hl, lumen del hepatopáncreas; hp, hepatopáncreas; lm, músculos longitudinales; ml, lumen del mesodeo; pm, membranas peritróficas.

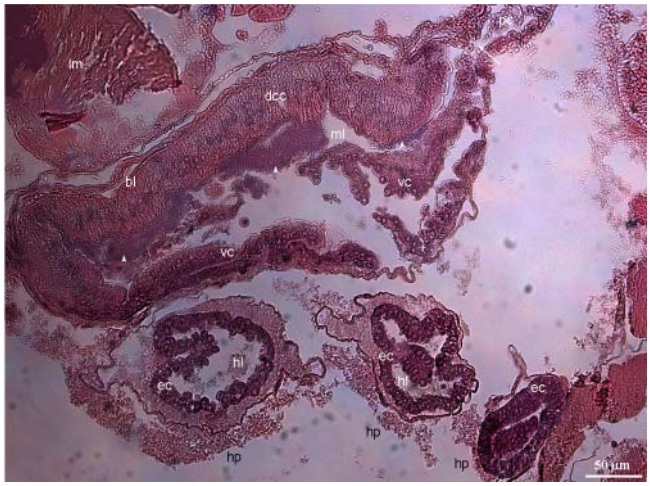

Fig. 14.—Transverse section of the posterior part of an empty midgut with the distal ends of the hepatopancreas of an adult male of *M. remyi*. Note the presumed secretion (arrowheads) in the midgut lumen and the opening of the posterior caecum (arrow) pointing in the opposite direction. bl, basal lamina; dcc, dorsal columnar cells; ec, E-cells; hl, hepatopancreatic lumen; hp, hepatopancreas; lm, longitudinal muscles; ml, midgut lumen; pc, posterior caeca; vc, ventral cuboidal cells.

Fig. 14.—Sección transversal de la parte posterior de un mesodeo vacío con el extremo distal del hepatopáncreas de un macho adulto de *M. remyi*. Se aprecia la secreción (puntas de flecha) en el lumen del mesodeo y la apertura del caecum posterior (flecha) apuntando en la dirección opuesta. bl, lámina basal; dcc, células de la columna dorsal; ec, células E; hl, lumen del hepatopáncreas; hp, hepatopáncreas; lm, músculos longitudinales; ml, lumen del mesodeo; pc, caeca posterior; vc, células cuboidales ventrales.

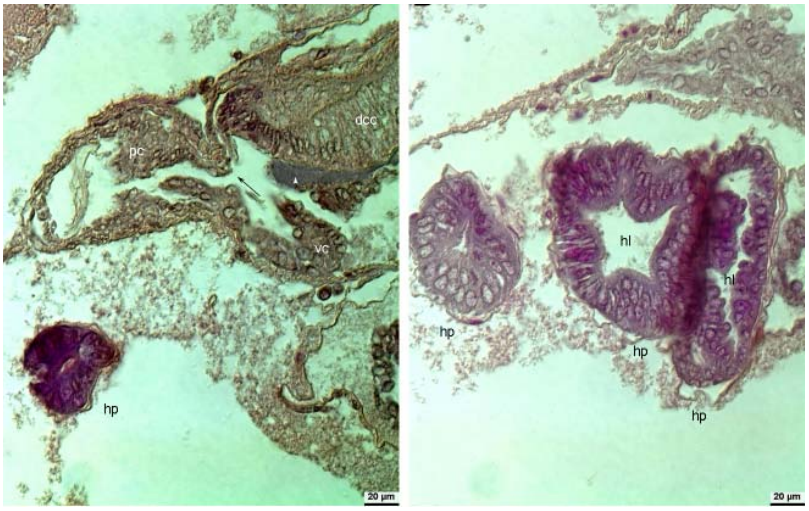

Fig. 15.—Magnification of the hepatopancreas and of the posterior caecum. The arrowhead indicates the secretion in the midgut lumen and the arrow indicates the entrance to the posterior caecum pointing in the opposite direction. dcc, dorsal columnar cells; hl, hepatopancreatic lumen; hp, hepatopancreas; pc, posterior caeca; vc, ventral cuboidal cells.

Fig. 15.—Magnificación del hepatopáncreas y del caecum posterior. Las puntas de flecha indican la secreción en el lumen del midgut y la flecha indica la entrada en el caecum posterior apuntando en la dirección opuesta. dcc, células de la columna dorsal; hl, lumen del hepatopáncreas; hp, hepatopáncreas; pc, caeca posterior; vc, células cuboidales ventrales.

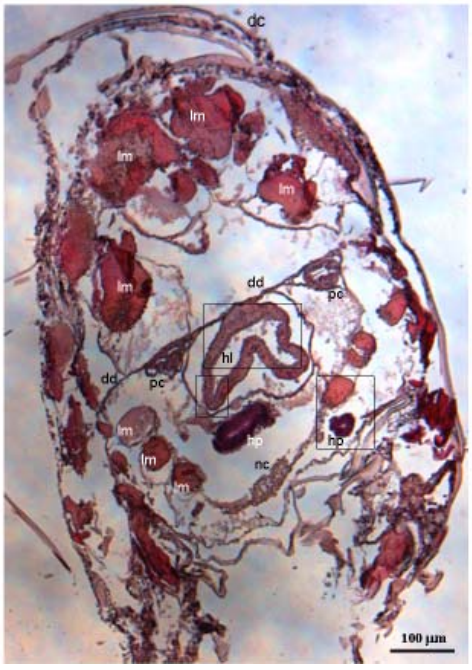

Fig. 16.—Transverse section of an anterior region of the hindgut of an adult male of *M. remyi*. dc, dorsal cuticle; dd, dorsal diaphragm; hl, hindgut lumen; hp, hepatopancreas; lm, longitudinal muscles; nc, nerve cord; pc, posterior caeca.

Fig. 16.—Sección transversal de la region anterior del proctodeo de un macho adulto de *M. remyi*. dc, cutícula dorsal; dd, diafragma dorsal; hl, lumen del proctodeo; hp, hepatopáncreas; lm, músculo longitudinal; nc, cordón nervioso; pc, caeca posterior.

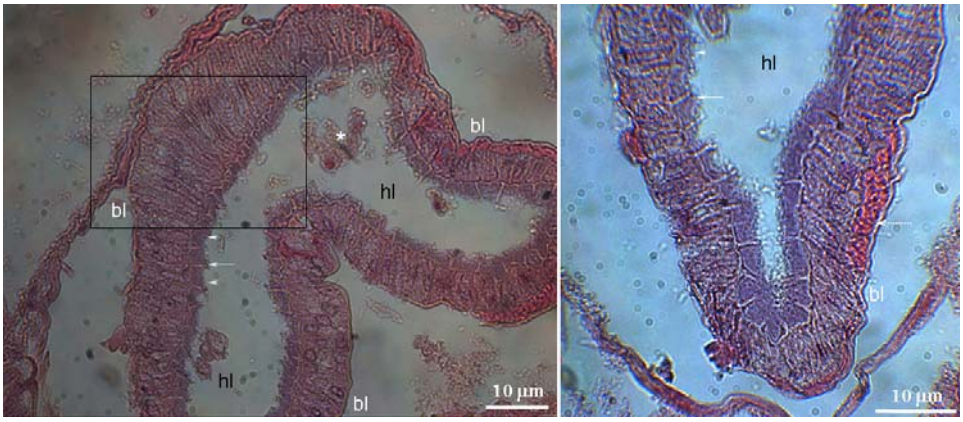

Fig. 17.—Magnification of the hindgut epithelium with the spines (arrows) covered by a presumed secretion (arrowheads) (see the rectangle within Fig. 16); note the plant fragments (asterisk) in the hindgut lumen and the presumed myoepithelial cells or muscle fibres (dotted arrow). bl, basal lamina; hl, hindgut lumen.
Fig. 17.—Magnificación del epitelio del proctodeo con las espinas (flechas) cubiertas de una secreción (puntas de flecha) (ver el rectángulo dentro de la Fig. 16); se aprecian los fragmentos de planta (asteriscos) en el lumen del proctodeo y el mioepitelio celular o las fibras de músculos (flecha punteada). bl, lamina basal; hl, lumen del proctodeo.

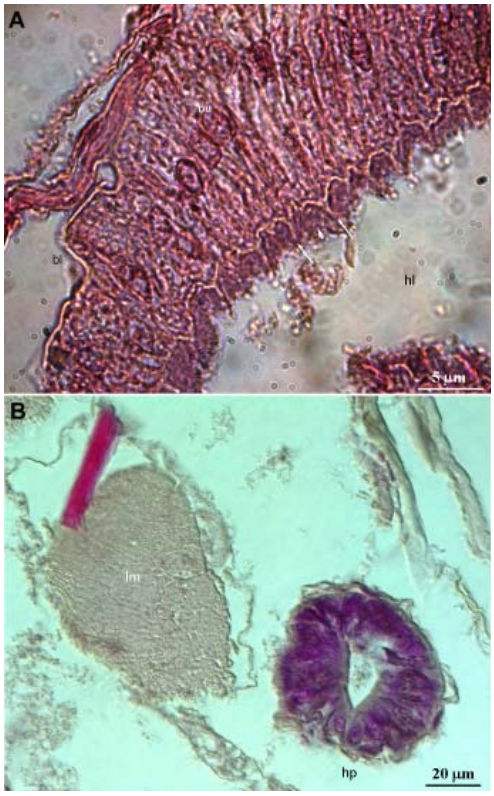

Fig. 18.—(A) Detail of the hindgut epithelium with the spines (arrows) covered by a presumed secretion (arrowheads) (see the rectangle within Fig. 17); (B) Magnification of the hepatopancreas (see the relative rectangle inside Fig. 16). bl, basal lamina; hl, hindgut lumen; hp, hepatopancreas; nu, nucleus.
Fig. 18.—(A) Detalle del epitelio del proctodeo con las espinas (flechas) cubiertas de una secreción (puntas de flecha) (ver el rectángulo dentro de la Fig. 17); (B) Magnificación del hepatopáncreas (ver el rectángulo relativo dentro de la Fig. 16). bl, lamina basal; hl, lumen del proctodeo; hp, hepatopáncreas; nu, núcleo.

Fig. 19.—Transverse section of a medial region of the hindgut of an adult male of *M. remyi*. bl, basal lamina; dd, dorsal diaphragm; em, extrinsic muscle; hl, hindgut lumen; lm, longitudinal muscles; nu, nucleus; pc, posterior caeca.
Fig. 19.—Sección transversal de la region medial del proctodeo de un macho adulto de *M. remyi*. bl, lámina basal; dd, diafragma dorsal; em, músculo extrínseco; hl, lumen del proctodeo; lm, músculos longitudinales; nu, núcleo; pc, caeca posterior.

Fig. 20.—Magnification of the hindgut epithelium. Note the spines (arrow) covered by a presumed secretion (arrowhead). dd, dorsal diaphragm; em, extrinsic muscle; hl, hindgut lumen; lm, longitudinal muscles; pc, posterior caeca.
Fig. 20.—Magnificación del epitelio del proctodeo. Se aprecian las espinas (flechas) cubiertas por una secreción (puntas de flecha). dd, diafragma dorsal; em, músculo extrínseco; hl, lumen del proctodeo; lm, músculos longitudinales; pc, caeca posterior.

Fig. 21.—Magnification of the hindgut epithelium (see the rectangle within Fig. 20). Note the presumed myoepithelial cells or muscle fibres (dotted arrows). bl, basal lamina; hl, hindgut lumen; nu, nucleus.
Fig. 21.— Magnificación del epitelio del proctodeo (ver el rectángulo dentro de la Fig. 20). Se aprecian las células del mioepitelio o fibras musculares (flechas punteadas). bl, lámina basal; hl, lumen del proctodeo; nu, núcleo.

Fig. 22.—Transverse section of a posterior region of the hindgut of an adult male of *M. remyi*. bl, basal lamina; dd, dorsal diaphragm; g, ganglion; hl, hindgut lumen; lm, longitudinal muscles; pa, posterior aorta; pc, posterior caeca.
Fig. 22.—Sección transversal de la region posterior del proctodeo de un macho adulto de *M. remyi*. bl, lamina basal; bb, diafragma dorsal; g, ganglio; hl, lumen del proctodeo; lm, músculos longitudinales; pa, aorta posterior; pc, caeca posterior.

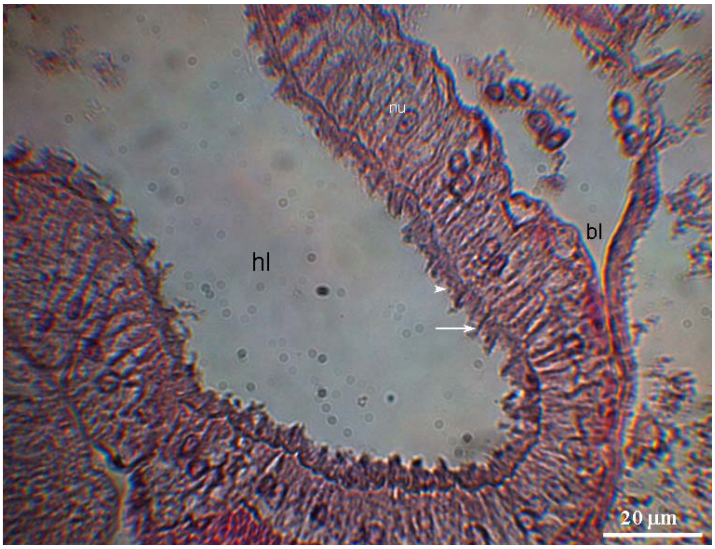

Fig. 23.—Magnification of the hindgut epithelium with the spines (arrow) covered by a presumed secretion (arrowhead) (see the rectangles within Fig. 22). bl, basal lamina; hl, hindgut lumen; nu, nucleus.
Fig. 23.—Magnificación del epitelio del proictodeo con las espinas (flechas) cubiertas de una secreación (puntas de flecha) (ver los rectángulos dentro de la Fig. 22). bl, lamina basal; hl, lumen del proctodeo; nu, núcleo.

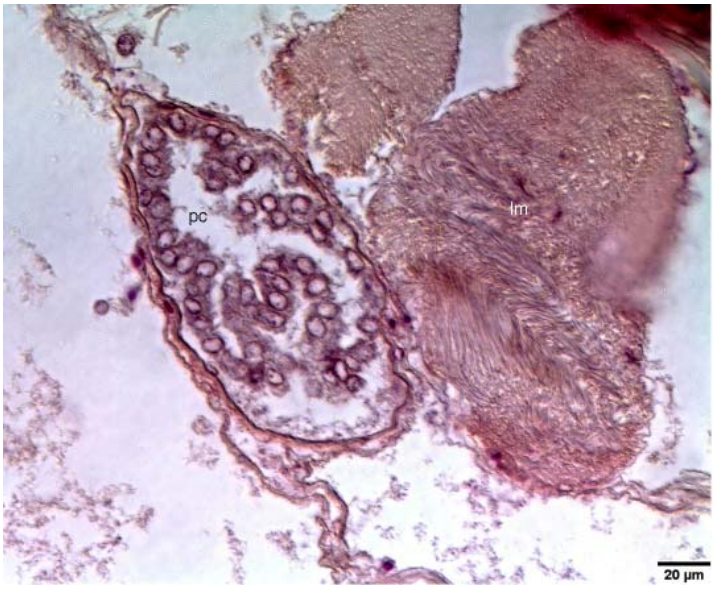

Fig. 24.—Magnification of the posterior caecum (see the rectangles within Fig. 22). lm, longitudinal muscles; pc, posterior caeca.
Fig. 24.—Magnificación del caecum posterior (ver los rectángulos dentro de la Fig. 22). lm, músculos longitudinales; pc, caeca posterior.